Original Article | Breast Imaging

eISSN 2005-8330
https://doi.org/10.3348/kjr.2023.0208
Korean J Radiol 2023;24(12):1190-1199

Korean Journal of Radiology
KJR

Ultrafast MRI and T1 and T2 Radiomics for Predicting Invasive Components in Ductal Carcinoma in Situ Diagnosed With Percutaneous Needle Biopsy

Min Young Kim[1,2,3], Heera Yoen[1], Hye Ji[1], Sang Joon Park[2,4], Sun Mi Kim[5], Wonshik Han[6], Nariya Cho[1,2,3]

[1]Department of Radiology, Seoul National University Hospital, Seoul, Republic of Korea
[2]Department of Radiology, Seoul National University College of Medicine, Seoul, Republic of Korea
[3]Institute of Radiation Medicine, Seoul National University Medical Research Center, Seoul, Republic of Korea
[4]MEDICALIP Co. Ltd., Seoul, Republic of Korea
[5]Department of Radiology, Seoul National University Bundang Hospital, Seoul National University College of Medicine, Seongnam, Republic of Korea
[6]Department of Surgery and Cancer Research Institute, Seoul National University Hospital, Seoul National University College of Medicine, Seoul, Republic of Korea

Objective: This study aimed to investigate the feasibility of ultrafast magnetic resonance imaging (MRI) and radiomic features derived from breast MRI for predicting the upstaging of ductal carcinoma in situ (DCIS) diagnosed using percutaneous needle biopsy.
Materials and Methods: Between August 2018 and June 2020, 95 patients with 98 DCIS lesions who underwent preoperative breast MRI, including an ultrafast sequence, and subsequent surgery were included. Four ultrafast MRI parameters were analyzed: time-to-enhancement, maximum slope (MS), area under the curve for 60 s after enhancement, and time-to-peak enhancement. One hundred and seven radiomic features were extracted for the whole tumor on the first post-contrast T1WI and T2WI using PyRadiomics. Clinicopathological characteristics, ultrafast MRI findings, and radiomic features were compared between the pure DCIS and DCIS with invasion groups. Prediction models, incorporating clinicopathological, ultrafast MRI, and radiomic features, were developed. Receiver operating characteristic curve analysis and area under the curve (AUC) were used to evaluate model performance in distinguishing between the two groups using leave-one-out cross-validation.
Results: Thirty-six of the 98 lesions (36.7%) were confirmed to have invasive components after surgery. Compared to the pure DCIS group, the DCIS with invasion group had a higher nuclear grade ($P < 0.001$), larger mean lesion size ($P = 0.038$), larger mean MS ($P = 0.002$), and different radiomic-related characteristics, including a more extensive tumor volume; higher maximum gray-level intensity; coarser, more complex, and heterogeneous texture; and a greater concentration of high gray-level intensity. No significant differences in AUCs were found between the model incorporating nuclear grade and lesion size (0.687) and the models integrating additional ultrafast MRI and radiomic features (0.680–0.732).
Conclusion: High nuclear grade, larger lesion size, larger MS, and multiple radiomic features were associated with DCIS upstaging. However, the addition of MS and radiomic features to the prediction model did not significantly improve the prediction performance.
Keywords: Breast; Neoplasms; Magnetic resonance imaging; Radiomics

INTRODUCTION

Breast ductal carcinoma in situ (DCIS) is a neoplasm confined to the ductal epithelium and bound by the basement membrane without invasion into the stromal tissue. With screening mammography, the incidence of DCIS has increased from 6% to 20% in newly diagnosed breast cancers over the last two decades [1,2]. Previously,

Received: August 18, 2022 **Revised:** July 26, 2023 **Accepted:** September 5, 2023
Corresponding author: Nariya Cho, MD, PhD, Department of Radiology, Seoul National University Hospital, 101 Daehak-ro, Jongno-gu, Seoul 03080, Republic of Korea
• E-mail: river7774@gmail.com

Korean Journal of Radiology
KJR

detection of DCIS was thought to prevent invasive cancer progression [3]. However, as only up to 40% of DCIS lesions progress to invasive tumors [4], clinical trials are underway to evaluate the outcomes of active surveillance instead of surgery with radiation therapy to avoid overtreatment issues [5-7]. Currently, because most patients with DCIS are diagnosed by core needle biopsy, the key to successful active surveillance is the precise preoperative identification of women at risk of upstaging to invasive cancers. A meta-analysis found that 26% of women with DCIS diagnosed by percutaneous needle biopsy had invasive cancer during surgery, and a smaller-gauge biopsy device, high nuclear grade, lesion size > 20 mm, and mammographic mass were associated with upstaging [8]. However, identifying invasive components based on core biopsy specimens is not sufficient for treatment decisions; thus, refined image analysis using three-dimensional magnetic resonance imaging (MRI) with high spatiotemporal resolution is needed.

Dynamic contrast-enhanced magnetic resonance imaging (DCE-MRI) is the most sensitive imaging modality for the detection of DCIS [9] and the most sophisticated imaging modality that reflects tumor heterogeneity [10]. On MRI, regional or temporal variations in signal intensity reflect the heterogeneity of vascularity, cell density, or metabolic activities of breast tumors, and regional or temporal signal intensity variations can be quantified. Quantification of MRI parameters based on radiomics is useful for differentiating between nuclear grades or human epidermal growth factor receptor 2 (HER2) status of DCIS [11] and molecular subtypes of invasive cancers [12-15]. Recently, several studies have been published in which radiomic features extracted from mammography [16,17] and preoperative MRI [18-20] may help predict the upstaging of DCIS. In addition, in terms of temporal signal intensity variations, very early kinetic information derived from ultrafast MRI, a technique for obtaining breast MRI with very high temporal resolution (4 to 7 s) within 1 min after contrast injection [21-23], has been shown to reflect histopathological characteristics. The time-to-enhancement (TTE) of breast tumors derived from ultrafast MRI distinguishes invasive tumors from DCIS [24-26].

To the best of our knowledge, few studies have been published on approaches to predict the invasive component of breast DCIS using a combination of ultrafast breast MRI and MRI radiomic analysis. Therefore, the purpose of our study was to retrospectively investigate the feasibility of ultrafast MRI and radiomic features derived from breast MRI for predicting the presence of invasive components in DCIS diagnosed using percutaneous needle biopsy.

MATERIALS AND METHODS

Case Selection

This retrospective study was approved by the Institutional Review Board of the Seoul National University Hospital, which waived the requirement for informed consent (IRB No. 2006-134-1133). Between August 2018 and June 2020, 110 consecutive patients diagnosed with DCIS by percutaneous needle biopsy, who underwent preoperative breast MRI, including ultrafast sequencing, were identified from the Breast Imaging Center database of Seoul National University Hospital. Among these patients, we excluded those who had not undergone subsequent surgery (n = 2), those who had a history of breast cancer surgery on the same side as the lesion (n = 2), and those who had undergone excisional biopsy before the MRI examination (n = 11). Finally, 95 patients (mean age ± standard deviation, 52.2 ± 9.9; range, 31–76 years) with 98 DCISs were included. Three patients had DCIS in bilateral breasts. Clinicopathological information was collected from medical records. The median interval between MRI examination and surgery was 33 days (range, 1–126 days).

MRI Techniques

MRI examinations were performed using a 3T MRI scanner (MAGNETOM Skyra, Siemens Healthineers GmbH). Ultrafast scans were acquired between a conventional pre-contrast axial T1-weighted scan and a conventional first post-contrast T1-weighted scan. After contrast injection, 17 series of ultrafast scans were acquired with 2.3 s of preparation time followed by 4.5 s per series. The total acquisition time for the ultrafast scans was 79 s. Other typical magnetic resonance (MR) scan protocols are described in the Supplementary Material, and the detailed MR parameters for ultrafast and conventional DCE-MRI are summarized in Table 1.

Image Analysis

Two radiologists (M.Y.K. and N.C., with 1 and 20 years of experience, respectively) evaluated conventional DCE-MRI and ultrafast MRI, respectively, in consensus. The radiologists were blinded to the surgical histopathological results. The lesion size and type were evaluated in the first post-contrast phase of conventional DCE-MRI to minimize the effect of background parenchymal enhancement. Lesion size was defined as the longest diameter of the enhancing tumor

 https://doi.org/10.3348/kjr.2023.0208

measured in three dimensions on MRI. The lesion type (mass and non-mass enhancement) was classified according to the breast imaging reporting and data system (BI-RADS) [27].

For the ultrafast MRI analysis, syngo.via Frontier (Siemens Healthineers) was used. The following four ultrafast scan parameters were calculated: TTE, maximum slope (MS), area under the curve for 60 s after enhancement (iAUC60), and time-to-peak enhancement (TTP) (Fig. 1). The detailed methods for analyzing the ultrafast scan parameters are described in the Supplementary Material.

Table 1. Acquisition parameters for ultrafast and conventional breast MRI

	Ultrafast	Conventional
Sequence	CS-VIBE	VIBE
TR, ms	3.91	4.7
TE, ms	1.54	1.7
Flip angle, degree	12	10
Field of view, mm^2	320 x 320	320 x 320
Matrix size	448 x 314	384 x 384
In-plane resolution, mm	0.7 x 0.7	0.83 x 0.83
Slice thickness, mm	0.8	1.0
Voxel volume, mm^3	0.39	0.64
Phase resolution, %	70	100
Slice resolution, %	50	75
Total acceleration factors	Compressed sensing: 24	CAIPIRINHA: 2 GRAPPA: 2
Number of dynamics	17	6 (1 pre, 5 post)
Temporal resolution, sec	4.5	88
Total acquisition time, min:sec	1:19	8:48

MRI = magnetic resonance imaging, CS-VIBE = compressed sensing volume-interpolated breath-hold examination, VIBE = volume-interpolated breath-hold examination, TR = repetition time, TE = echo time, CAIPIRINHA = controlled aliasing in parallel imaging results in higher acceleration, GRAPPA = generalized auto-calibrating partially parallel acquisition

Tumor Segmentation and Radiomic Feature Extraction

For radiomic analysis, tumor segmentation was performed by two radiologists (M.Y.K. and N.C., with 1 and 20 years of experience, respectively) in consensus. The necrotic, hemorrhagic, and cystic areas of the tumor were avoided using T2-weighted image (T2WI) and subtraction imaging. Digital imaging and communications in medicine (DICOM) MRI files were exported from the picture archiving and communication system (PACS) and loaded into the MEDIP Research v2.1.1 software (MEDICALIP). A region of interest (ROI) was manually drawn along the tumor boundary on every slice of the first post-contrast T1-weighted image (T1WI) of conventional DCE-MRI to include the whole tumor volume and was saved as an ROI mask file (Fig. 2). The resolution of the ROI mask file was adjusted using ImageJ because the resolutions of T1WI and T2WI were different. After adjusting the resolution, the ROI mask file for each lesion was pasted to the T2WI, and additional manual editing of the ROI on T2WI was not performed, except for positioning.

Radiomic features were automatically extracted from each ROI on T1WI and T2WI in the radiomics module of MEDIP Research v2.1.1 (MEDICALIP), which reproduces the formula of PyRadiomics (pyradiomics.readthedocs.io) [28] (Fig. 2).

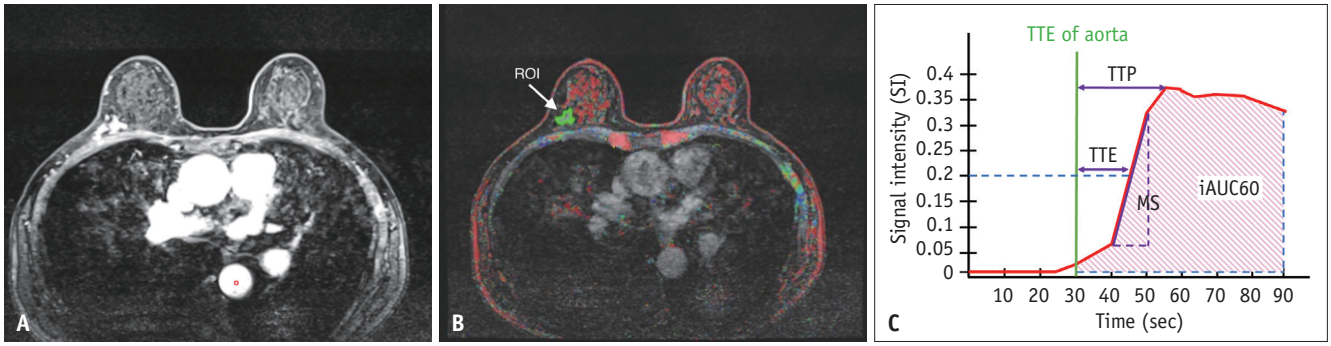

Fig. 1. Acquisition of parameters at ultrafast MRI. **A:** A 64-year-old female with DCIS with invasive ductal carcinoma. As a reference, a circular region of interest (ROI) was placed in the descending thoracic aorta in the first series of ultrafast scans. **B:** The tumor ROI (arrow) was manually drawn along the margin of the fastest enhancing area of the entire tumor in the right upper outer breast. **C:** The software program automatically calculated the four parameters in the ultrafast scan after plotting the signal intensity of the ROIs according to time; time-to-enhancement (TTE) was the time to reach 20% relative enhancement and was calculated by subtracting the aorta TTE from the tumor TTE. The maximum slope (MS) was calculated from the maximum average slope of the relative enhancement between two time points. iAUC60 was the area under the curve for 60 s after aorta TTE. Time-to-peak enhancement (TTP) was calculated by subtracting the aorta TTE from the time at which the tumor ROI showed peak enhancement. MRI = magnetic resonance imaging, DCIS = ductal carcinoma in situ, iAUC60 = area under the curve for 60 s after enhancement

https://doi.org/10.3348/kjr.2023.0208

Korean Journal of Radiology
KJR

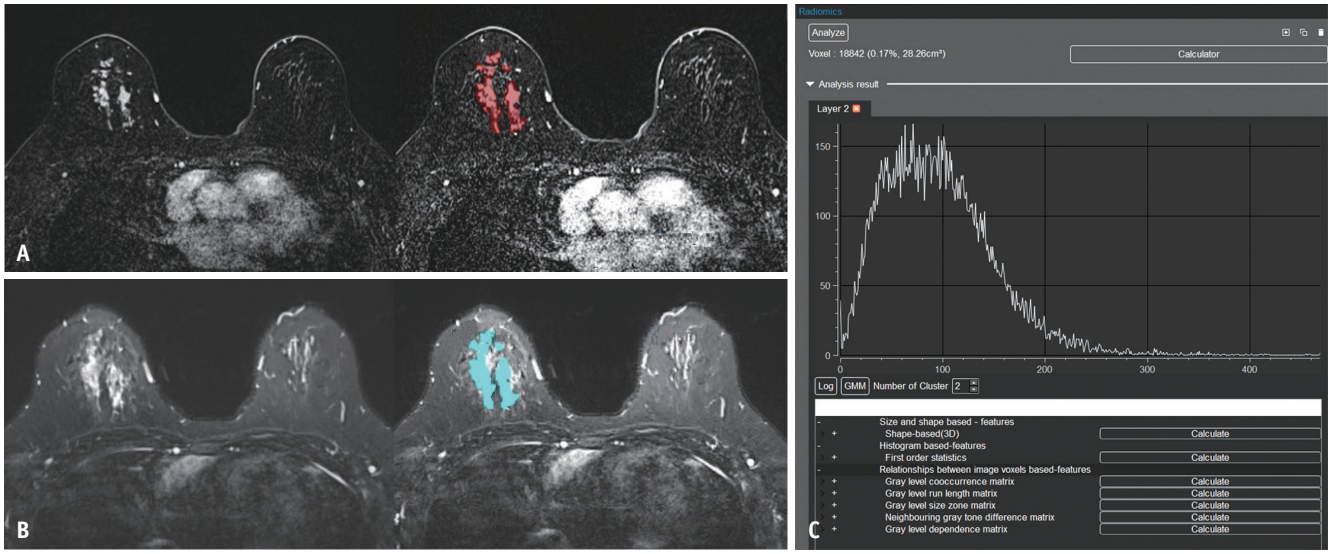

Fig. 2. Radiomic analysis of conventional MRI. **A:** A 57-year-old female with ductal carcinoma in situ (DCIS) and invasive ductal carcinoma of the right breast. After the DICOM file was loaded into the program, the region of interest (ROI) was manually drawn along the tumor boundary on every slice of the first post-contrast T1WI of conventional DCE-MRI (red figures). **B:** The ROI mask file of the entire tumor was copied and pasted in the correct position on the T2WI (blue figures). **C:** The radiomics module of the program automatically calculated 107 radiomic features of the seven classes. MRI = magnetic resonance imaging, DICOM = digital imaging and communications in medicine, T1WI = T1-weighted image, DCE-MRI = dynamic contrast-enhanced magnetic resonance imaging, T2WI = T2-weighted image

A total of 107 radiomic features of 7 classes were extracted including 3-dimensional (3D) shape-based features (n = 14), first-order features (n = 18), gray-level co-occurrence matrix features (GLCM, n = 24), gray-level run-length matrix features (GLRLM, n = 16), gray-level size-zone matrix features (GLSZM, n = 16), neighbouring gray-tone difference matrix features (NGTDM, n = 5), and gray-level dependence matrix features (GLDM, n = 14). First-order features represent the distribution of gray-level intensities within an ROI. The other five classes, except for 3D shape-based features, are second- or higher-order statistics about the gray-level intensities and mutual positions of voxels in the ROI describing textures. The detailed definition and calculation formula for the radiomic features can be accessed at https://pyradiomics.readthedocs.io/en/latest/features.html.

Radiomic Feature Selection

Before radiomic feature selection, all radiomic features were standardized with a zero mean and one standard deviation. Least absolute shrinkage and selection operator (LASSO) regression was performed to select radiomic features that could predict invasive cancer. The optimal lambda value was chosen when the area under the curve (AUC) of the receiver operating characteristic (ROC) analysis was the highest through 7-fold cross-validation, and radiomic features with non-zero coefficients were selected at that lambda value (Supplementary Fig. 1). LASSO regression was performed on each of the 107 radiomic features extracted from T1WI and T2WI and on 214 radiomic features combining T1WI and T2WI. Subsequently, the 'radiomics score' was calculated from the selected radiomic features. The equation for calculating the 'radiomics score' is described in Supplementary Material, and the selected radiomic features are shown in Supplementary Table 1.

Prediction Model Construction and Internal Validation

For the prediction of invasive cancer among patients with DCIS diagnosed by percutaneous needle biopsy, five prediction models were constructed through logistic regression using different combinations of clinicopathological information, ultrafast and conventional MRI features, and radiomics scores from LASSO regression.

Clinicopathological information and ultrafast and conventional MRI features were compared between the DCIS with invasion and the pure DCIS groups. For continuous variables, an independent *t*-test or a Mann-Whitney U test was performed. For categorical variables, Pearson's chi-square test was used. Variables with P value < 0.05 were entered into the logistic regression.

Each prediction model was evaluated using a leave-

 https://doi.org/10.3348/kjr.2023.0208

one-out cross-validation (LOOCV). The performance of the prediction model was assessed using the AUC with a 95% confidence interval (CI). DeLong's test was used to compare the AUCs of different models.

Statistical Analysis

Statistical analysis was performed using R statistical software (version 4.0.3; R Foundation for Statistical Computing) and IBM SPSS version 25.0. A *P* value < 0.05 indicated statistical significance. Considering the exploratory nature of this study, adjustments for multiple comparisons were not made.

RESULTS

Patients and Tumor Characteristics

Patient and tumor characteristics are summarized in Table 2. Of the 98 lesions, 36 (36.7%) had invasive components on surgical histopathology, and 62 (63.3%) were pure DCIS. No difference was found between the DCIS with invasion and pure DCIS groups in terms of mean age (*P* = 0.705), presence of symptoms (*P* = 0.093), biopsy method (*P* = 0.094), or time interval from MR scan to surgery (*P* = 0.445).

According to the histopathological results, the DCIS with invasion group had a higher nuclear grade than the pure DCIS group (66.7% [24/36] vs. 27.4% [17/62], *P* < 0.001). The median size of the invasive components of the DCIS with invasion group was 0.3 cm (range: < 0.05 cm to 2.5 cm).

Table 2. Patient and tumor characteristics

	Pure DCIS (n = 62)	DCIS with invasion (n = 36)	*P*
Age, yr	52 ± 10 (34–75)	53 ± 10 (31–76)	0.705
Symptom			0.093
No	52 (83.9)	25 (69.4)	
Yes*	10 (16.1)	11 (30.6)	
Palpable	5 (8.1)	7 (19.4)	
Nipple discharge	4 (6.4)	6 (16.7)	
Pain	1 (1.6)	1 (2.8)	
Biopsy method			0.094
CNB	40 (64.5)	29 (80.6)	
VAB	22 (35.5)	7 (19.4)	
Nuclear grade			< 0.001
1 or 2	45 (72.6)	12 (33.3)	
3	17 (27.4)	24 (66.7)	
Time interval, day†	34 (1–73)	29 (6–126)	0.445

Data are mean ± standard deviation (range) for age, median (range) for time interval, and number (percentage) for others.
*Three patients in the DCIS with invasion group complained of more than one symptom, †Time interval from MR scan to surgery.
DCIS = ductal carcinoma in situ, CNB = core needle biopsy, VAB = vacuum-assisted biopsy, MR = magnetic resonance

Conventional and Ultrafast MRI Features According to Surgical Histopathology

Table 3 compares the conventional and ultrafast MRI features between the DCIS with invasion group and the pure DCIS group. The mean lesion size measured on MRI was larger in the DCIS with invasion group than in the pure DCIS group (4.1 ± 2.9 vs. 2.9 ± 1.9 cm, *P* = 0.038). The mean MS of the DCIS with invasion group was larger than the mean MS of the pure DCIS group (1161.9 ± 431.3 vs. 911.0 ± 356.5, *P* = 0.002) (Figs. 3, 4). No differences were found in the lesion type, TTE, iAUC60, or TTP between the two groups.

Radiomic Feature Analysis

One hundred and seven radiomic features were extracted from the T1WIs and T2WIs. Individual radiomic features were compared between the DCIS with invasion and pure DCIS groups (Supplementary Tables 2, 3). When each radiomic feature was interpreted according to the definition in PyRadiomics (pyradiomics.readthedocs.io), the DCIS with invasion group showed a more extensive tumor volume; higher maximum gray-level intensity; coarser, more complex, and heterogeneous texture patterns; and a greater concentration of high gray-level intensity than the pure DCIS group.

Table 3. Conventional and ultrafast MRI features according to surgical histopathology

	Pure DCIS (n = 62)	DCIS with invasion (n = 36)	*P*
Lesion size, cm*	2.9 ± 1.9 (0.6–8)	4.1 ± 2.9 (0.8–12.7)	0.038
Lesion type			0.474
Mass	23 (37.1)	16 (44.4)	
NME	39 (62.9)	20 (55.6)	
Ultrafast DCE-MRI parameters			
TTE	10.8 ± 5.1	9.2 ± 4.7	0.119
MS	911.0 ± 356.5	1161.9 ± 431.3	0.002
iAUC60	127.9 ± 34.8	128.7 ± 33.0	0.911
TTP	56.6 ± 16.5	52.9 ± 14.3	0.262

Data are mean ± SD (range) for lesion size, number (percentage) for lesion type, and mean ± SD for ultrafast MRI parameters.
*Longest length of the lesion measured on MRI.
MRI = magnetic resonance imaging, DCIS = ductal carcinoma in situ, NME = non-mass enhancement, DCE = dynamic contrast enhancement, TTE = time-to-enhancement, MS = maximum slope, iAUC60 = area under the curve for 60 s after enhancement, TTP = time-to-peak enhancement, SD = standard deviation

https://doi.org/10.3348/kjr.2023.0208

Korean Journal of Radiology
KJR

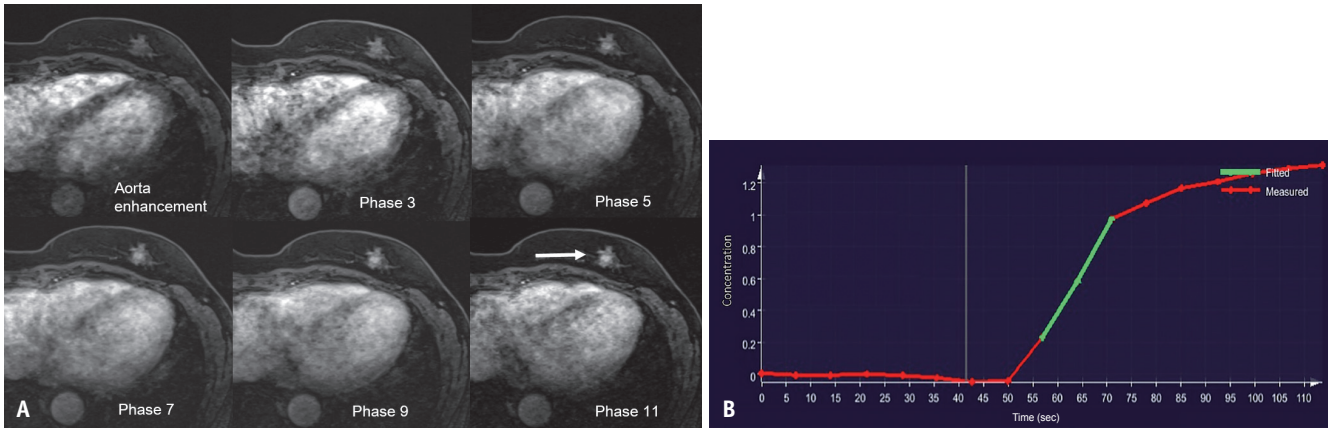

Fig. 3. A 59-year-old female with pure ductal carcinoma in situ (DCIS). **A:** Ultrafast DCE-MRI shows a 3.7-cm segmental non-mass enhancement (arrow) in the left lower breast. Surgical histopathology confirmed that the lesion consisted of a 1.3-cm DCIS component. **B:** Time-intensity curve of the ultrafast MRI of the lesion. The time-to-enhancement (TTE) was 14.794 s, maximum slope (MS) was 560.704 s, area under the curve for 60 s after enhancement (iAUC60) was 103.182 s, and time-to-peak enhancement (TTP) was 67.52 s. DCE-MRI = dynamic contrast-enhanced magnetic resonance imaging, MRI = magnetic resonance imaging

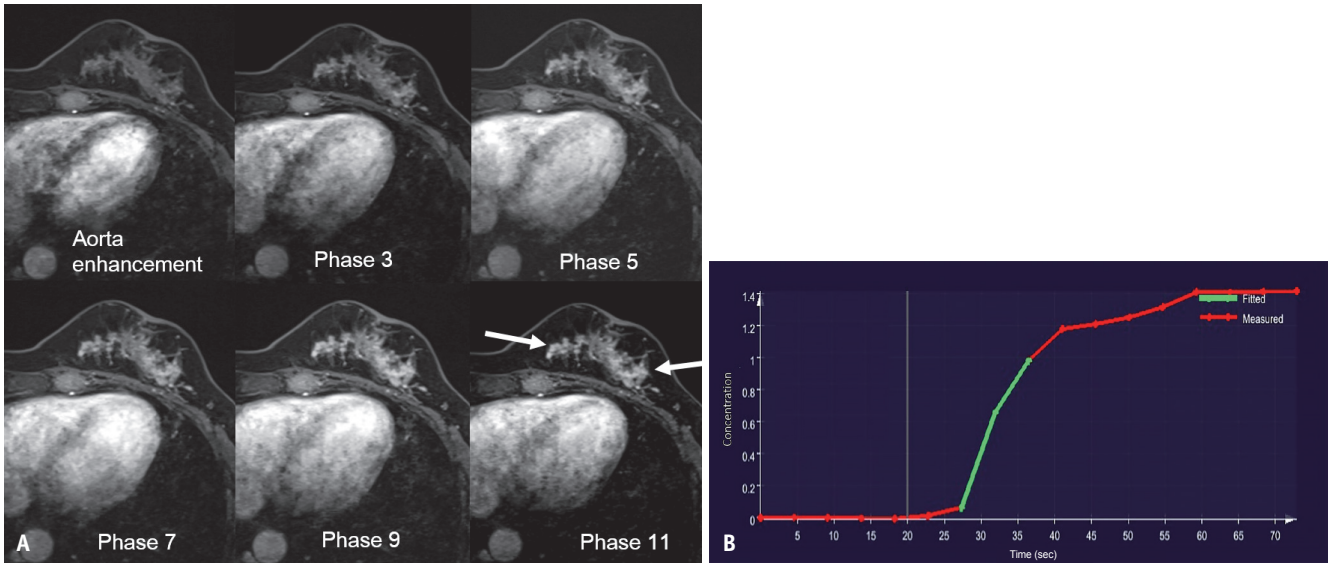

Fig. 4. A 51-year-old female with ductal carcinoma in situ (DCIS) with invasive ductal carcinoma. **A:** Ultrafast DCE-MRI shows an 8.3-cm non-mass enhancement (arrows) in the left breast. Surgical histopathology confirmed that the lesion consisted of a 0.3-cm invasive component and a 7.8-cm DCIS component. **B:** Time-intensity curve of the ultrafast MRI of the lesion. The time-to-enhancement (TTE) was 8.132 s, maximum slope (MS) was 1021.915, area under the curve for 60 s after enhancement (iAUC60) was 108.657, and time-to-peak enhancement (TTP) was 46.741 s. DCE-MRI = dynamic contrast-enhanced magnetic resonance imaging, MRI = magnetic resonance imaging

However, the number of radiomic features was large, they showed multicollinearity, and the meaning of individual features was often ambiguous. Therefore, feature selection was performed using LASSO regression. After LASSO regression, ten radiomic features were selected from T1WI, three radiomic features were selected from T2WI, and eight radiomic features were selected from the combination of T1WI and T2WI. The 'radiomics score' was calculated using selected radiomic features (Supplementary Table 1).

Discrimination Performance Evaluation of Prediction Models

Based on the results of the aforementioned analysis, five models were constructed to predict the invasive components of DCIS. M1 was constructed using the nuclear grade and lesion size measured on MRI (referred to as the clinical model). M2 was created using the ultrafast MRI feature MS along with the variables used in M1. M3, M4, and M5 were created using the variables used in M2 and the 'radiomics

 https://doi.org/10.3348/kjr.2023.0208

Table 4. Discrimination performance of five models for predicting invasive components in DCIS

Model	AUC*	$P^{\dagger}$	$P^{\ddagger}$
M1 (Clinical): Nuclear grade + Lesion size	0.687 (0.569–0.805)	0.162	0.586
M2: Clinical + Ultrafast MRI MS	0.732 (0.625–0.839)	-	0.995
M3: Clinical + MS + T1WI radiomics	0.724 (0.611–0.836)	0.915	0.806
M4: Clinical + MS + T2WI radiomics	0.680 (0.563–0.797)	0.520	0.257
M5: Clinical + MS + T1WI + T2WI radiomics	0.732 (0.622–0.841)	0.995	-

The data in parentheses are 95% confidence intervals.
*AUCs of each prediction model using leave-one-out cross-validation (LOOCV), †The result of comparing the AUCs of the five prediction models with M2 as the gold standard using DeLong's test, ‡The result of comparing the AUCs of the five prediction models with M5 as the gold standard using DeLong's test.
DCIS = ductal carcinoma in situ, AUC = area under the receiver operating characteristic curve, MRI = magnetic resonance imaging, MS = maximum slope, T1WI = T1-weighted image, T2WI = T2-weighted image

score' which was calculated from the selected radiomic features of T1WI, T2WI, and their combination, respectively.

The AUCs obtained using LOOCV for the five models are listed in Table 4. Models M2 and M5 had the highest point estimate AUCs of 0.732 (95% CI, 0.625–0.839 for M2; 0.622–0.841 for M5). However, when the AUCs of the prediction models were compared, there was no statistically significant difference in performance.

DISCUSSION

Preoperative prediction of DCIS upstaging is crucial for management decisions, such as omitting sentinel lymph node biopsy or determining the eligibility for active surveillance. Our study found that the group upstaged to invasive ductal carcinoma (IDC) at surgery had a higher nuclear grade, larger lesion size on MRI, larger MS on ultrafast MRI, and more heterogeneous and coarser radiomic texture on T1WI and T2WI. The prediction model using clinical features and MS and the prediction model using clinical, MS, and radiomic features showed higher point-estimate AUC values than the model using clinical features only; however, there was no significant difference in model performance.

High nuclear grade is a well-known preoperative risk factor for upstaging DCIS diagnosed using percutaneous needle biopsy [8]. Therefore, the eligibility criteria for ongoing active surveillance trials include only low- or intermediate-nuclear-grade DCIS [5-7]. Our results further emphasized this association by demonstrating that the DCIS with invasion group had a higher nuclear grade than the pure DCIS group.

The association between larger lesion size and upstaging of DCIS in our study is consistent with previous studies in which a larger tumor size was associated with DCIS with invasive cancer [8,29,30], which might be explained by the increased likelihood of missing an invasive focus during core needle biopsy for a larger tumor. Sentinel lymph node biopsy is usually considered for patients with large (> 2 cm), high-grade DCIS [31], and our results support this finding.

Regarding ultrafast MRI parameters, shorter TTE or larger MS have been shown to be associated with invasive cancer or aggressive tumor characteristics such as high grade, hormone receptor negativity, or high Ki-67 levels [24,26,32]. Recent studies have reported that TTE or MS can help predict DCIS upgrade [30,33]. In line with these studies, we also found that the MS in the DCIS with invasion group was larger than that in the pure DCIS group. The association between larger MS and invasive components in DCIS could be explained by increased microvessel density and vessel permeability triggered by tumor-induced angiogenesis, which is associated with tumor enhancement on MRI [34-36]. Mori et al. [37] also reported that the initial slope of enhancement on ultrafast DCE-MRI, similar to MS in our study, significantly correlated with the histological microvessel density of IDC. In addition, the onset of an angiogenic switch was known to occur during the invasive progression of DCIS [38]. These results indicate that DCIS with invasive components may have increased microvessel density, leading to a larger MS. Therefore, MS could be used as an imaging biomarker to predict the upstaging of DCIS, if validated in future studies.

Concerning radiomic analysis, the DCIS with invasion group showed higher gray-level intensities and a more heterogeneous and coarser texture than the pure DCIS group. As mentioned earlier, increased microvessel density in the DCIS with invasion group likely contributed to the higher gray-level intensities on the first post-contrast T1WI. According to previous studies, intratumoral heterogeneity has been detected in DCIS [4,39], which aids in the adaptation to stressful and selective forces during tumor

https://doi.org/10.3348/kjr.2023.0208

Korean Journal of Radiology
KJR

progression [40]. Therefore, we believe that DCIS with higher intratumoral heterogeneity is more likely to progress and appear as a heterogeneous texture on radiomic analysis.

With regard to the performance of the prediction models, adding MS or radiomic features to the clinical model did not significantly improve prediction performance. Previous studies on the prediction models for DCIS upstaging have reported various results. Similar to our findings, Miceli et al. reported no significant performance improvement using ultrafast MRI [33]. Another study insisted that the AUC of lesion size, MS, and maximum enhancement were higher than the AUC of each feature alone; however, they did not provide *P* values [30]. Regarding the addition of radiomic features, Hong et al. [18] and Wu et al. [20] reported a statistically significant performance improvement in the combined model compared with the clinical model. However, contrary to our research, they analyzed only one slice of MRI showing the largest cross-sectional area of the lesion, or included patients with DCIS appearing as non-mass enhancement only on MRI. Therefore, different inclusion criteria and image segmentation methods may have affected the results.

This study had several limitations. First, we used LOOCV for the cross-validation of the prediction models. The idea behind LOOCV is to use one sample as the validation set and the others as the training set and repeat this process for each sample in the dataset. Therefore, the validation set was not independent of the training set, and LOOCV may have overestimated model performance. Second, visual assessment of the fastest enhancing portion on ultrafast MRI and manual tumor segmentation for radiomic analysis were performed by two radiologists in consensus. We did not evaluate the intra- and interobserver agreement for the measurements. Therefore, the measurement values could vary depending on the researcher, which might affect the reproducibility of our study results. Third, our study was a single-center retrospective analysis, which limits the generalizability of the results.

In conclusion, the DCIS with invasion group had a higher nuclear grade, larger lesion size, larger MS on ultrafast MRI, higher signal intensities, and more heterogeneous and coarser texture on post-contrast T1WI and T2WI of conventional MRI than the pure DCIS group. However, the prediction model using clinical features combined with MS or radiomic features did not clearly show an improved performance in predicting DCIS upstaging. Considering the labor-intensive nature of radiomic analysis and the similar performances of adding MS and adding both MS and radiomic features, adding MS alone may be a practical option. However, further research and validation are required to confirm the usefulness of our findings.

Supplement

The Supplement is available with this article at https://doi.org/10.3348/kjr.2023.0208.

Availability of Data and Material

The datasets generated or analyzed during the study are not publicly available due to patient-related data but are available from the corresponding author on reasonable request.

Conflicts of Interest

Sang Joon Park is founder and CEO of MEDICALIP, however, this do not affect the publication of this manuscript. All remaining authors have declared no conflicts of interest.

Author Contributions

Conceptualization: Min Young Kim, Nariya Cho. Data curation: Min Young Kim, Nariya Cho. Formal analysis: Min Young Kim. Investigation: Min Young Kim, Heera Yoen, Hye Ji, Nariya Cho. Software: Sang Joon Park. Supervision: Nariya Cho. Writing—original draft: Min Young Kim. Writing—review & editing: Min Young Kim, Nariya Cho, Sun Mi Kim, Wonshik Han.

ORCID IDs

Min Young Kim
https://orcid.org/0000-0002-9354-2890
Heera Yoen
https://orcid.org/0000-0001-5583-6065
Hye Ji
https://orcid.org/0000-0001-8268-0043
Sang Joon Park
https://orcid.org/0000-0003-1013-681X
Sun Mi Kim
https://orcid.org/0000-0003-0899-3580
Wonshik Han
https://orcid.org/0000-0001-7310-0764
Nariya Cho
https://orcid.org/0000-0003-4290-2777

Funding Statement

None

REFERENCES

1. Esserman L, Yau C. Rethinking the standard for ductal carcinoma in situ treatment. *JAMA Oncol* 2015;1:881-883
2. Korean Breast Cancer Society. *Breast cancer facts & figures 2020*. Seoul: Korean Breast Cancer Society, 2020:8-9
3. Cady B. How to prevent invasive breast cancer: detect and excise duct carcinoma in situ. *J Surg Oncol* 1998;69:60-62
4. Cowell CF, Weigelt B, Sakr RA, Ng CK, Hicks J, King TA, et al. Progression from ductal carcinoma in situ to invasive breast cancer: revisited. *Mol Oncol* 2013;7:859-869
5. Elshof LE, Tryfonidis K, Slaets L, van Leeuwen-Stok AE, Skinner VP, Dif N, et al. Feasibility of a prospective, randomised, open-label, international multicentre, phase III, non-inferiority trial to assess the safety of active surveillance for low risk ductal carcinoma in situ - The LORD study. *Eur J Cancer* 2015;51:1497-1510
6. Francis A, Thomas J, Fallowfield L, Wallis M, Bartlett JM, Brookes C, et al. Addressing overtreatment of screen detected DCIS; the LORIS trial. *Eur J Cancer* 2015;51:2296-2303
7. Hwang ES, Hyslop T, Lynch T, Frank E, Pinto D, Basila D, et al. The COMET (Comparison of Operative versus Monitoring and Endocrine Therapy) trial: a phase III randomised controlled clinical trial for low-risk ductal carcinoma in situ (DCIS). *BMJ Open* 2019;9:e026797
8. Brennan ME, Turner RM, Ciatto S, Marinovich ML, French JR, Macaskill P, et al. Ductal carcinoma in situ at core-needle biopsy: meta-analysis of underestimation and predictors of invasive breast cancer. *Radiology* 2011;260:119-128
9. Greenwood HI, Wilmes LJ, Kelil T, Joe BN. Role of breast MRI in the evaluation and detection of DCIS: opportunities and challenges. *J Magn Reson Imaging* 2020;52:697-709
10. Alic L, Niessen WJ, Veenland JF. Quantification of heterogeneity as a biomarker in tumor imaging: a systematic review. *PLoS One* 2014;9:e110300
11. Chou SS, Gombos EC, Chikarmane SA, Giess CS, Jayender J. Computer-aided heterogeneity analysis in breast MR imaging assessment of ductal carcinoma in situ: correlating histologic grade and receptor status. *J Magn Reson Imaging* 2017;46:1748-1759
12. Ko ES, Kim JH, Lim Y, Han BK, Cho EY, Nam SJ. Assessment of invasive breast cancer heterogeneity using whole-tumor magnetic resonance imaging texture analysis: correlations with detailed pathological findings. *Medicine (Baltimore)* 2016;95:e2453
13. Chang RF, Chen HH, Chang YC, Huang CS, Chen JH, Lo CM. Quantification of breast tumor heterogeneity for ER status, HER2 status, and TN molecular subtype evaluation on DCE-MRI. *Magn Reson Imaging* 2016;34:809-819
14. Sutton EJ, Oh JH, Dashevsky BZ, Veeraraghavan H, Apte AP, Thakur SB, et al. Breast cancer subtype intertumor heterogeneity: MRI-based features predict results of a genomic assay. *J Magn Reson Imaging* 2015;42:1398-1406
15. Lee SH, Park H, Ko ES. Radiomics in breast imaging from techniques to clinical applications: a review. *Korean J Radiol* 2020;21:779-792
16. Li J, Song Y, Xu S, Wang J, Huang H, Ma W, et al. Predicting underestimation of ductal carcinoma in situ: a comparison between radiomics and conventional approaches. *Int J Comput Assist Radiol Surg* 2019;14:709-721
17. Hou R, Grimm LJ, Mazurowski MA, Marks JR, King LM, Maley CC, et al. Prediction of upstaging in ductal carcinoma in situ based on mammographic radiomic features. *Radiology* 2022;303:54-62
18. Hong M, Fan S, Yu Z, Gao C, Fang Z, Du L, et al. Evaluating upstaging in ductal carcinoma in situ using preoperative MRI-based radiomics. *J Magn Reson Imaging* 2023;58:454-463
19. Lee HJ, Park JH, Nguyen AT, Do LN, Park MH, Lee JS, et al. Prediction of the histologic upgrade of ductal carcinoma in situ using a combined radiomics and machine learning approach based on breast dynamic contrast-enhanced magnetic resonance imaging. *Front Oncol* 2022;12:1032809
20. Wu Z, Lin Q, Wang H, Wang G, Fu G, Bian T. An MRI-based radiomics nomogram to distinguish ductal carcinoma in situ with microinvasion from ductal carcinoma in situ of breast cancer. *Acad Radiol* 2023;30 Suppl 2:S71-S81
21. Mann RM, Mus RD, van Zelst J, Geppert C, Karssemeijer N, Platel B. A novel approach to contrast-enhanced breast magnetic resonance imaging for screening: high-resolution ultrafast dynamic imaging. *Invest Radiol* 2014;49:579-585
22. Mus RD, Borelli C, Bult P, Weiland E, Karssemeijer N, Barentsz JO, et al. Time to enhancement derived from ultrafast breast MRI as a novel parameter to discriminate benign from malignant breast lesions. *Eur J Radiol* 2017;89:90-96
23. Kim SY, Cho N, Choi Y, Shin SU, Kim ES, Lee SH, et al. Ultrafast dynamic contrast-enhanced breast MRI: lesion conspicuity and size assessment according to background parenchymal enhancement. *Korean J Radiol* 2020;21:561-571
24. Goto M, Sakai K, Yokota H, Kiba M, Yoshida M, Imai H, et al. Diagnostic performance of initial enhancement analysis using ultra-fast dynamic contrast-enhanced MRI for breast lesions. *Eur Radiol* 2019;29:1164-1174
25. Heacock L, Lewin AA, Gao Y, Babb JS, Heller SL, Melsaether AN, et al. Feasibility analysis of early temporal kinetics as a surrogate marker for breast tumor type, grade, and aggressiveness. *J Magn Reson Imaging* 2018;47:1692-1700
26. Shin SU, Cho N, Kim SY, Lee SH, Chang JM, Moon WK. Time-to-enhancement at ultrafast breast DCE-MRI: potential imaging biomarker of tumour aggressiveness. *Eur Radiol* 2020;30:4058-4068
27. American College of Radiology. *ACR BI-RADS(R) Atlas. Breast Imaging Reporting and Data System*. 5th ed. Reston: American College of Radiology, 2013
28. van Griethuysen JJM, Fedorov A, Parmar C, Hosny A, Aucoin N, Narayan V, et al. Computational radiomics system to decode the radiographic phenotype. *Cancer Res* 2017;77:e104-e107
29. Lamb LR, Lehman CD, Oseni TO, Bahl M. Ductal carcinoma in situ (DCIS) at breast MRI: predictors of upgrade to invasive

https://doi.org/10.3348/kjr.2023.0208

carcinoma. *Acad Radiol* 2020;27:1394-1399
30. Heo S, Park AY, Jung HK, Ko KH, Kim Y, Koh J. The usefulness of ultrafast MRI evaluation for predicting histologic upgrade of ductal carcinoma in situ. *Eur J Radiol* 2021;136:109519
31. El Hage Chehade H, Headon H, Wazir U, Abtar H, Kasem A, Mokbel K. Is sentinel lymph node biopsy indicated in patients with a diagnosis of ductal carcinoma in situ? A systematic literature review and meta-analysis. *Am J Surg* 2017;213:171-180
32. Onishi N, Sadinski M, Hughes MC, Ko ES, Gibbs P, Gallagher KM, et al. Ultrafast dynamic contrast-enhanced breast MRI may generate prognostic imaging markers of breast cancer. *Breast Cancer Res* 2020;22:58
33. Miceli R, Gao Y, Qian K, Heller SL. Predicting upgrade of ductal carcinoma in situ to invasive breast cancer at surgery with ultrafast imaging. *AJR Am J Roentgenol* 2023;221:34-43
34. Gilles R, Zafrani B, Guinebretiere JM, Meunier M, Lucidarme O, Tardivon AA, et al. Ductal carcinoma in situ: MR imaging-histopathologic correlation. *Radiology* 1995;196:415-419
35. Hulka CA, Edmister WB, Smith BL, Tan L, Sgroi DC, Campbell T, et al. Dynamic echo-planar imaging of the breast: experience in diagnosing breast carcinoma and correlation with tumor angiogenesis. *Radiology* 1997;205:837-842
36. Oshida K, Nagashima T, Ueda T, Yagata H, Tanabe N, Nakano S, et al. Pharmacokinetic analysis of ductal carcinoma in situ of the breast using dynamic MR mammography. *Eur Radiol* 2005;15:1353-1360
37. Mori N, Abe H, Mugikura S, Takasawa C, Sato S, Miyashita M, et al. Ultrafast dynamic contrast-enhanced breast MRI: kinetic curve assessment using empirical mathematical model validated with histological microvessel density. *Acad Radiol* 2019;26:e141-e149
38. Bluff JE, Menakuru SR, Cross SS, Higham SE, Balasubramanian SP, Brown NJ, et al. Angiogenesis is associated with the onset of hyperplasia in human ductal breast disease. *Br J Cancer* 2009;101:666-672
39. Vincent-Salomon A, Lucchesi C, Gruel N, Raynal V, Pierron G, Goudefroye R, et al. Integrated genomic and transcriptomic analysis of ductal carcinoma in situ of the breast. *Clin Cancer Res* 2008;14:1956-1965
40. Sinha VC, Piwnica-Worms H. Intratumoral heterogeneity in ductal carcinoma in situ: chaos and consequence. *J Mammary Gland Biol Neoplasia* 2018;23:191-205

 https://doi.org/10.3348/kjr.2023.0208